

Optical Magnetometry

Dmitry Budker^{1,2,*} and Michael Romalis^{3,†}

¹*Department of Physics, University of California, Berkeley, CA 94720-7300*

²*Nuclear Science Division, Lawrence Berkeley National Laboratory, Berkeley CA 94720*

³*Department of Physics, Princeton University, Princeton, NJ 08544*

(Dated: November 26, 2024)

Some of the most sensitive methods of measuring magnetic fields utilize interactions of resonant light with atomic vapor. Recent developments in this vibrant field are improving magnetometers in many traditional areas such as measurement of geomagnetic anomalies and magnetic fields in space, and are opening the door to new ones, including, dynamical measurements of bio-magnetic fields, detection of nuclear magnetic resonance (NMR), magnetic-resonance imaging (MRI), inertial-rotation sensing, magnetic microscopy with cold atoms, and tests of fundamental symmetries of Nature.

PACS numbers:

I. MEASURING MAGNETIC FIELDS WITH ATOMS AND LIGHT

It has been nearly half a century since the techniques of measuring magnetic fields using optical pumping and probing of alkali atoms were realized in the pioneering work of Dehmelt [1], Bell and Bloom [2, 3] and further developed by Cohen-Tannoudji, Dupon-Roc, and co-workers, see, for example, Refs. [4, 5]. The general idea of the method is that light which is near-resonant with an optical transition creates long-lived orientation and/or higher order moments in the atomic ground state that subsequently undergo Larmor spin precession in the magnetic field. This precession modifies the optical absorptive and dispersive properties of the atoms and this modification is detected by measuring the light transmitted through the atomic medium. Recent reviews of resonant magneto-optics have been given in Refs. [6, 7].

The fields of resonant magneto-optics and atomic magnetometry have been experiencing a new boom driven by technological developments, specifically by the advent of reliable, small, inexpensive, and easily tunable diode lasers on the one hand, and by the refinement of the techniques of producing dense atomic vapors with long (in some cases ~ 1 s) ground-state relaxation times on the other. These technical advances have enabled atomic magnetometers to achieve sensitivities rivaling [8, 9, 10, 11] and even surpassing [12] that of most Superconducting Quantum Interference Device (SQUID) based magnetometers that have dominated the field of sensitive magnetometers for a number of years [13]. Atomic magnetometers have the intrinsic advantage of not requiring cryogenic cooling, and offer a significant potential for miniaturization. In contrast to SQUIDs that measure magnetic flux through a pick-up loop, atomic magnetometers measure magnetic field directly. Atomic

magnetometers can be configured so that their output is related to the magnitude of the magnetic field through fundamental physical constants, so that no calibration is required.

Presently, the most sensitive atomic optical magnetometer is the spin-exchange-relaxation-free (SERF) magnetometer whose demonstrated sensitivity exceeds 10^{-15} T/ $\sqrt{\text{Hz}}$, with projected fundamental limits below 10^{-17} T/ $\sqrt{\text{Hz}}$ [12]. SERF magnetometers also offer a possibility of spatially-resolved measurements with millimeter resolution.

The present-day interest in optical magnetometers is driven by numerous and diverse applications, a partial list of which includes tests of the fundamental symmetries of Nature, search for man-made and natural magnetic anomalies, investigation of the dynamics of the geomagnetic fields (including attempts at earthquake prediction), material science and investigation of magnetic properties of rocks, detection of magnetic microparticles at ultra-low concentrations, detection of signals in nuclear magnetic resonance (NMR) and magnetic-resonance imaging (MRI), direct detection of magnetic fields from the heart and the brain, magnetic microscopy, and measuring magnetic fields in space.

In this paper, we outline the basic principles and fundamental limits of the sensitivity of optical atomic magnetometers, and discuss several specific applications.

II. GENERAL FEATURES AND LIMITS OF SENSITIVITY OF OPTICAL MAGNETOMETERS

A general schematic of an optical atomic magnetometer is shown in Fig. 1. In many magnetometers, the resonant medium is a vapor of alkali atoms (Rb, Cs, or K) contained in a glass bulb. Because atomic polarization is generally destroyed when atoms collide with the walls of the bulb, cells filled with buffer gas are commonly used. The gas ensures that the atoms optically polarized in the central part of the cell take a long time to diffuse to the walls. Another technique for reducing wall relax-

*Electronic address: budker@berkeley.edu

†Electronic address: romalis@princeton.edu

ation is application of a non-relaxing coating, typically, paraffin, on the cell walls (see below). As mentioned above, the light sources of choice today are diode lasers; however, discharge lamps – the original light sources for atomic magnetometers – are still used in most commercial atomic magnetometers, and can achieve sensitivity comparable to lasers in some research applications [14]. Figure 1 shows separate light sources for pumping and probing with orthogonal light beams. There exist many magnetometer configurations that differ by relative direction and spectral tuning of the pump and probe light. In some schemes, pumping and probing is performed by the same beam. The two most common detection modes are monitoring the intensity and polarization of the transmitted probe light. The latter method has certain intrinsic advantages, such as its ability to detect very small polarization-rotation angles, and a reduced sensitivity to the laser-intensity noise. Shown in Fig. 1 is an all-optical magnetometer; no other electromagnetic fields are applied to the atoms apart from the magnetic field being measured and the pump and probe light. Some magnetometers require additional means for excitation of spin precession. A weak magnetic field oscillating at the Larmor frequency is commonly used for this purpose [2, 10]. Other techniques include application of microwave fields [15] and all-optical excitation using various types of modulation of the light beams: intensity, frequency or polarization [3, 7].

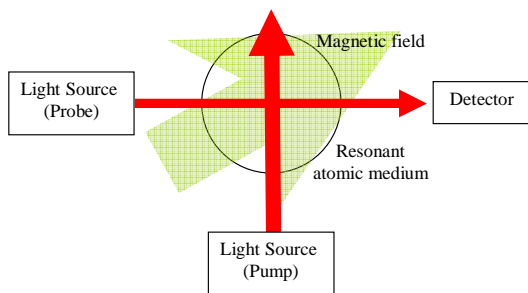


FIG. 1: A general schematic of an all-optical atomic magnetometer. Pump light polarizes the atoms, atomic polarization evolves in the magnetic field, and the resultant state of the atoms' polarization is detected by measuring transmission or polarization rotation of the probe light.

Quantum mechanics sets fundamental limits on the best sensitivity that can be achieved in a magnetic-field measurement using atoms. One such limit is associated with projection noise resulting from the fact that if an atom is polarized in a particular direction, a measurement of the angular-momentum projection m on an orthogonal direction yields a random result ($+1/2$ or $-1/2$ in the simplest case of angular momentum $F = 1/2$). Ignoring factors of order unity that depend on particulars of the system (for example, the total value of the angular momentum F , and the relative contributions of different Zeeman sublevels), the sensitivity of a magnetic-field measurement performed for a time T with an ensemble

of N atoms with coherence time τ is

$$\delta B \simeq \frac{1}{g\mu_B} \frac{\hbar}{\sqrt{N\tau T}}, \quad (1)$$

where μ_B is the Bohr magneton, g is the ground-state Landé factor, and \hbar is the Planck's constant. Equation (1) is derived by noticing that a measurement with a single atom with a duration of τ produces an uncertainty in the Larmor precession angle on the order of 1 rad. With N atoms, this is improved by \sqrt{N} , and repeating the measurement multiple times gains another factor of $\sqrt{T/\tau}$.

Recently, a possibility of overcoming the projection noise in magnetometry using spin-squeezing techniques – where quantum states are prepared with unequal distribution of uncertainty between conjugate observables, in this case, the projections of the angular momentum on two orthogonal directions – was discussed and demonstrated (see Ref. [16] and references therein). Unfortunately, an improvement in sensitivity using spin squeezing appears possible only on a time scale significantly shorter than the spin-relaxation time [17].

In optical magnetometry, in addition to the atomic projection noise, there is also photon shot noise. For example, if the measured quantity is the rotation angle φ of the light polarization, the shot noise is

$$\delta\varphi_s \simeq \frac{1}{2\sqrt{\dot{N}_{ph}T}}. \quad (2)$$

Here \dot{N}_{ph} is the probe-photon flux (in photons/s) after the atomic sample. Depending on the details of a particular measurement, either the spin noise (1) or the photon noise (2) may dominate. However, if a measurement is optimized for statistical sensitivity, the two contributions to the noise are generally found to be comparable [11, 18].

Another potential source of noise in atomic magnetometers is the AC Stark shift caused by the probe and/or pump laser, which generates a fictitious magnetic field proportional to the degree of circular polarization of the light [19]. Even in the absence of technical sources of intensity or polarization fluctuations, quantum fluctuations generate noise of the fictitious magnetic field [20]. However, the noise due to AC Stark shifts can, in principle, be eliminated by choosing a laser frequency where it crosses zero [21] or a geometry where the fictitious field is orthogonal to the measured magnetic field. Nevertheless, in practical implementations of magnetometers, light shifts due to drifts of laser properties are often a significant concern.

The ultimate sensitivity of atomic magnetometers is given by the product of three quantities in Eq. (1), the magnetic moment of the atoms ($g\mu_B$), the square root of the number of atoms involved in the measurement, and the square root of the spin-relaxation time. Consequently, to improve the sensitivity of a magnetometer, the number of atoms in the system and their spin-relaxation time should be maximized.

There are several mechanisms that limit spin-relaxation time, one of the most important being depolarization caused by collisions with the cell walls that enclose the atomic vapor. Surface relaxation can be reduced by using a coating that has a low adsorption energy for atoms, so they spend less time bound to the surface of the cell. Among such coatings, paraffin and other materials with long chains of hydrocarbons were found to work well with alkali metals [22]. In a seminal study [23] Bouchiat and Brossel demonstrated that spin relaxation on paraffin is caused by two effects of comparable size, magnetic dipolar interaction and spin-rotation coupling. Magnetic dipolar relaxation is dominated by interaction between the magnetic moment of the electron and magnetic moments of protons in the coating. They showed that replacing hydrogen with deuterium, which has about three times smaller nuclear magnetic moment, reduces this type of relaxation. Despite work by several groups over the years, surface coating is still a rather laborious process with some degree of “black magic” that does not always yield reproducible results. While collisions with bare glass are generally completely depolarizing for alkali atoms, high-quality coatings can allow more than 10,000 bounces before depolarization, which also implies that even if a small fraction of the surface has defects, this will ruin the performance of the coating.

Another way to improve magnetometer sensitivity is to increase the density of alkali-metal atoms, as was studied, for example, in Ref. [24]. This typically requires increasing the temperature of the cell, although alternative approaches using light-induced desorption have been investigated [25]. Since paraffin coatings do not work at temperatures higher than $\approx 80^\circ\text{C}$, high-density magnetometers usually use a buffer gas to slow down the diffusion of alkali-metal atoms to cell walls. Slow atomic diffusion combined with spatially resolved optical detection also allows many independent measurements of the magnetic field inside one cell [12]. As the density is increased, at some point, the spin relaxation time becomes dominated by collisions between alkali-metal atoms and the product $N\tau$ approaches a constant, so that shot-noise sensitivity no longer increases with density. Thus, relaxation due to collisions between alkali-metal atoms represents a fundamental obstacle to improvement in sensitivity for a given cell volume.

Collisions between alkali-metal atoms are dominated by the spin-exchange process in which the electron spins of the colliding atoms rotate with respect to their combined spin, which is conserved in the collision. Even though such collisions conserve the total spin, they can lead to loss of spin coherence. All alkali atoms have non-zero nuclear spin, I , and their ground states are split into two hyperfine-structure components, characterized by the total angular momentum $F = I \pm 1/2$. The direction of magnetic precession, determined by the relative orientation of the electron spin with respect to the total angular momentum, is opposite for the two hyperfine states. Thus, in the presence of a magnetic field, the

spin-exchange collisions that randomly transfer atoms between the two hyperfine states normally lead to spin-relaxation, as atomic angular momenta acquire random angles with respect to each other.

As was first realized by Happer [26, 27], it is possible to suppress the effects of spin-exchange relaxation by *increasing* the rate of spin-exchange collisions until it exceeds the Larmor precession frequency. The effect is quite similar to Dicke narrowing [28] in microwave and optical spectroscopy or motional narrowing in NMR. In the rapid spin-exchange regime, we may no longer speak of magnetic precession of atoms in an individual hyperfine state. Instead, each atom experiences an average precession in the same direction as would a free atom in the $F = I + 1/2$ state. This is because atoms, while being redistributed among the sublevels, spend more time in this state, which has a higher statistical weight and higher electron-spin polarization. As a result, in a weak external magnetic field, the average angular momentum of the atomic vapor precesses without spin-exchange relaxation, although at a rate that is slower than the precession rate for a free atom. The slowing down of the spin precession rate depends on the distribution of atoms among magnetic sublevels and is thus a sensitive function of the optical pumping process [29]. This dependence on local optical pumping conditions may lead to non-uniformity of the spin precession frequency over the volume of the cell and broadening of the resonance signal. The problem can be avoided by operating the magnetometer near zero magnetic field.

In this regime the Zeeman resonance linewidth is not broadened at all by spin-exchange collisions and the alkali metal density can be increased to about 10^{14} cm^{-3} , four orders of magnitude higher than in traditional atomic magnetometers. Eventually the relaxation time becomes limited by “spin-destruction” collisions between alkali-metal atoms that do not conserve the total spin of the colliding pair. Several mechanisms of comparable importance have been identified for such relaxation [30], but some aspects of this process remain poorly understood [31]. The measured spin-destruction cross-sections are smaller for lighter alkali-metal atoms and result in a fundamental limit on the sensitivity of a K magnetometer of about $10^{-17}V^{-1/2}\text{ T/Hz}^{1/2}$ [32], where V is the active volume of the sensor in cm^3 .

The spin-exchange-relaxation-free regime can be achieved only in a magnetic field range of less than about 10 nT. At higher magnetic fields such as the Earth’s field, it is possible to use a single SERF magnetometer as a 3-axis null-detector with external feedback [33]. The possibility of reducing spin-exchange relaxation in a finite magnetic field has also been explored [34]. The idea is to pump most atoms into a stretched state with $m = I + 1/2$ where they cannot undergo spin-exchange collisions due to conservation of angular momentum. This technique works at any magnetic field, but it cannot completely eliminate spin-exchange relaxation, since a high optical pumping rate required to put atoms into the stretched

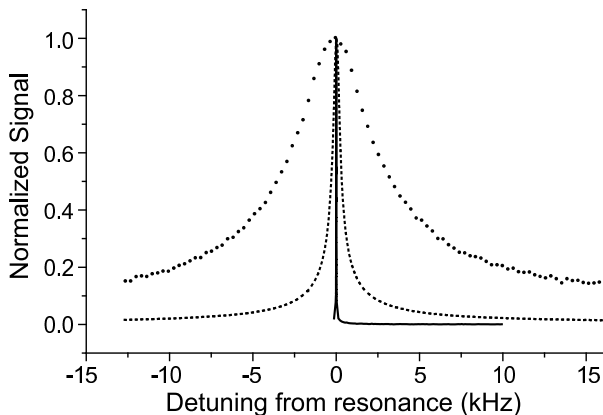


FIG. 2: Comparison of Zeeman resonances for different modes of operation in a potassium vapor with density $n = 7 \times 10^{13} \text{ cm}^{-3}$. Points: Spin-exchange broadened resonance with a full width at half maximum of 3 kHz observed in a magnetic field of $10 \text{ } \mu\text{T}$ when spin polarization is low. Dashed line: Resonance is narrowed to a full width of 350 Hz at the same magnetic field by pumping a large fraction of atoms into a stretched state parallel to the magnetic field. Solid line: At a field of 5 nT, the resonance width is 2 Hz due to complete elimination of spin-exchange broadening in the the rapid spin-exchange regime. (Adapted from Ref. [18].)

spin state in the presence of other relaxation processes also contributes to the resonance linewidth. For an optimal pumping rate the minimum resonance linewidth is given by the geometric mean of the spin-exchange and spin-destruction rates [18, 35]. This method for reduction of spin-exchange broadening has been used for narrowing of a microwave resonance in an alkali-metal atomic clock [35] and to improve the sensitivity of a resonant magnetometer for detection of very weak RF fields [18]. However, this technique does not significantly improve the sensitivity for measurements of static fields because excitation of large spin coherences, necessary to obtain an optimal signal/noise ratio, removes the atoms from the stretched spin state [36].

In Fig. 2 we show the Zeeman resonance curves obtained in a dense alkali-metal vapor in three different regimes. Spin-exchange broadening for low spin polarization is reduced by a factor of 10 by pumping most atoms into a stretched spin state. The linewidth can be further reduced by a factor of more than 100 in a very low magnetic field, where spin-exchange relaxation is completely eliminated.

III. ADDITIONAL CHARACTERISTICS OF A MAGNETOMETER

Apart from sensitivity, there are many other characteristics of a magnetometer that are important for specific applications. We have already mentioned that some of the most sensitive magnetometers operate best at relatively small magnetic fields, i.e., they have a lim-

ited *dynamic range*. An important benchmark for the magnetometer's dynamic range is the geomagnetic field $\sim 50 \text{ } \mu\text{T}$ of interest in many applications. While traditional rf-optical double resonance magnetometers have operated in this range from their inception (see, for example, Ref. [37]), diode-laser-based all-optical magnetometers for the geophysical range have been also developed recently (Refs. [38, 39, 40, 41], for example). At geomagnetic fields, sensitive atomic magnetometers have to contend with the complications arising from the nonlinear Zeeman effect caused by the Breit-Rabi mixing of hyperfine energy levels. The nonlinear Zeeman effect leads to a splitting of the magnetic resonance into multiple lines (see, for example, Ref. [39]). Several approaches have been proposed to alleviate the adverse effects of the nonlinear Zeeman effect in all-optical magnetometers, including synchronous optical pumping at the quantum revival frequency given by the quadratic correction to the Zeeman energies (Ref. [42] and references therein), and selective excitation and detection of coherences (that correspond to high-order polarization multipoles) between “stretched” Zeeman sublevels unaffected by nonlinear Zeeman effect [43, 44, 45].

Another important property of a magnetometer is whether it is *scalar* or *vector*, i.e., whether it measures the total magnitude, or specific cartesian component(s) of the magnetic field. While knowing all three vector components of a field provides a more complete information about the field, a truly scalar sensor has an advantage in that the device is insensitive to the orientation of the sensor with respect to the field, which is important for operation on a mobile platform.

Many magnetometer applications require operation at frequencies lower than 1 Hz where $1/f$ noise is often dominant. Atomic magnetometers have an intrinsic advantage over other types of sensors in this regard because they use a sensing element with very simple structure that does not generate intrinsic $1/f$ noise usually observed in solid-state systems with many nearly degenerate energy states [46]. In practical situations, significant $1/f$ noise may arise due to external elements, such as laser fluctuations caused by air currents. Such noise may be reduced using spin modulation techniques [47].

Atomic magnetometers operating in a finite field naturally tend to be of the scalar type as they rely on the resonance between an rf field or a modulated light field with Zeeman-split energy eigenstates of an atom. However, there is a standard technique (see, for example, Refs. [33, 48, 49]) for converting a scalar sensor into a vector one that relies on the fact that if a small bias field is applied to the sensor in a certain direction in addition to the field to be measured, then the change in the overall field magnitude is linear in the projection of the bias field on the main field, and is only quadratic (and generally negligible) in the projection on the orthogonal plane. Thus, applying three orthogonal bias fields consecutively, and performing three measurements of the overall magnetic-field magnitude, one reconstructs the overall field vector.

In practice, it may be convenient to apply all three bias fields simultaneously and modulate them at different frequencies. Synchronous detection of the magnetometer output at a corresponding frequency yields the value of the cartesian component of the magnetic field being measured.

For practical operation at finite fields, atomic magnetometers require a feedback loop to keep the frequency of the excitation locked to resonance as the magnetic field is changing. One approach is to use a phase-sensitive detector with an external feedback loop and a voltage-controlled oscillator. Another approach, which is often simpler, is a *self-oscillating* magnetometer that uses the measured spin-precession signal to directly generate the rf-field in a positive feedback loop [37]. All-optical self-oscillating atomic magnetometers have been demonstrated recently, utilizing transitions between hyperfine [50] and Zeeman sublevels [51, 52].

An important characteristic of a magnetometer is how fast the device responds to a change in the magnetic field. The time response of a passive atomic magnetometer to a small variation in the magnetic field is usually equivalent to a first-order low-pass filter with a time constant τ . Hence the natural bandwidth of such a magnetometer is equal to $(2\pi\tau)^{-1}$ Hz. If it is desirable to make measurements on a time scale $T < \tau$, one can adjust the operating parameters of the magnetometer, such as the probe beam intensity, so $\tau = T$. If the number of atoms N is fixed, then according to Eq. (1), one loses in sensitivity as T^{-1} for short times. However, if the number of alkali atoms can be increased and the spin-coherence time is limited by collisions between alkali atoms, then the sensitivity decreases only as $T^{-1/2}$. With fixed number of atoms and light power, it is possible to increase the bandwidth of a magnetometer with external feedback by using a large gain in the feedback loop. However, if the bandwidth is increased by a factor K over the natural bandwidth, the magnetometer output noise also increases by the same factor K [53].

It is also interesting to consider the response of a magnetometer to an instantaneous change in the magnetic field. Since Larmor precession has no inertia, a magnetometer based on such precession responds instantaneously to a change in the field. Our knowledge of the new value of the frequency will be at first very uncertain, but will improve with time as $T^{3/2}$ (the best scaling for the uncertainty of a single-tone-frequency determination from a noisy signal [54]). This is discussed in the context of a practical self-oscillating magnetometer in Ref. [52], where the effect of additional noise sources such as photodetector and amplifier noise are also considered.

In the case of portable and space-borne magnetometers, important characteristics include “heading errors” – the dependence of the reading of the magnetometer on the orientation of the sensor with respect to the field being measured, as well as the existence of “dead zones,” i.e., spatial orientations where the magnetometer loses its sensitivity. Other parameters of importance in-

clude size and power consumption of the sensor system. A recent trend is utilization of vertical-cavity surface-emitting lasers (VCSEL) as light sources which provide on the order of a milliwatt of light resonant with the D-lines of rubidium and cesium, do not require an external cavity, and consume only a few milliwatts of power. Miniaturization of the vapor cells to millimeter scales can be done using more or less standard techniques (see, for example, Ref. [55] for a description of a prototype optical-rotation magnetometer using a 3-mm diameter paraffin-coated Cs cell). Another approach, particularly appealing for future mass production of miniaturized low-cost magnetometers, is manufacturing of an integrated sensor package incorporating a VCSEL laser, an alkali-vapor cell, optics, and a detector using the wafer production techniques well developed by the semi-conductor industry. The first magnetometers based on this approach with a grain-of-rice sized integrated sensor have been recently constructed [56, 57], demonstrating a sensitivity of $50 \text{ pT}/\sqrt{\text{Hz}}$, with anticipated improvement by several orders of magnitude with further optimization.

A favorable feature of magnetometers with a small vapor cell is their reduced sensitivity to magnetic-field gradients that can lead to additional spin relaxation, line broadening, and performance degradation. Magnetometers utilizing buffer-gas free anti-relaxation coated cells are also less sensitive to small field gradients, because each atom samples the volume of the cell during its many bounces between the walls in the course of a relaxation time. This leads to a significant averaging of the magnetic-field inhomogeneities. A systematic study of the effects of the gradients on the Rb ground-state spin relaxation in a coated cell is presented in Ref. [58] along with a survey of earlier work.

IV. APPLICATIONS

A. Biological magnetic fields

Detection of magnetic fields of biological origin allows non-invasive studies of the time dependence and spatial distribution of biocurrents. Most biological magnetic field studies have focused on detection of the fields from the heart and the brain. Measurements of the magnetic fields generated by the heart (magnetocardiography) provide richer diagnostic information about heart function than traditional electrocardiography and do not require placing electrical contacts on the patient [59]. Useful diagnostic information is obtained by measuring the spatial distribution of the magnetic field during different parts of the heart cycle. Most magnetocardiography studies have been performed in magnetically shielded rooms, but they are considered too expensive for clinical application, and widespread use of magnetocardiography requires development of relatively low-cost sensors that can operate in unshielded environment. Measuring magnetic fields generated by the brain (magnetoencephalography) has

been used extensively for functional brain studies [60]. Magnetic fields associated with a particular sensory input, such as auditory, visual or tactile stimulation, are recorded by averaging the signals over many presentations of the same stimulus. Detailed measurements of the spatial distribution of the magnetic field around the head allows one to identify regions of the brain that become active during processing of the sensory input. However, spatial localization is complicated by the fact that the inverse problem of finding the current distribution responsible for a particular magnetic field distribution does not have a unique solution. Additional information, such as MRI data and sophisticated numerical algorithms are used for spatial localization. Magnetoencephalography also finds increasing use in clinical diagnostic applications, for example for treatment of epilepsy [61].

The first measurements of biological fields with an atomic magnetometer were performed in the 70s [62] but this approach was not widely pursued and the majority of biomagnetic applications relied on SQUID magnetometers. Recent progress in atomic magnetometry has again attracted interest in their application for measurements of biological magnetic fields with non-cryogenic sensors. Figure 3 shows examples of magnetic fields from the heart and the brain detected with atomic magnetometers. The cardio-magnetometer is based on optical-rf double resonance and uses Cs atoms at 30°C, allowing it to be placed close to a human body [63]. Cardiomagnetic fields are recorded sequentially on a grid of points above human chest. Measurements of the brain magnetic field have been performed with a potassium SERF magnetometer which operates at the vapor cell temperature of 180°C and uses a multi-channel photodetector to simultaneously record the spatial distribution of the magnetic fields [64]. Even though heating is required to maintain the operating temperature of the cell positioned close to the subject's head, it is technically easier and cheaper to do than maintaining cryogenic temperature at the sensor, as required in the case of SQUIDS.

B. Fundamental applications

Many fundamental interactions reduce at low energy to a spin coupling similar to magnetic interaction since the spin is the only vector available in the rest frame of the particle. Atomic magnetometers are intrinsically sensitive probes of the spin precession and hence play an important role in tests of fundamental symmetries. An example of the magnetometers' versatile nature is a Cs magnetometer constructed at Amherst. It was used to set a limit on parity (P) and time-reversal invariance (T) violating electron electric dipole moment (EDM) d that generates $d\vec{E} \cdot \vec{S}$ coupling [65], on violation of Lorentz invariance manifested as a spin coupling $\vec{b} \cdot \vec{S}$ to a background vector field \vec{b} [66], and on spin-dependent forces that can be mediated by axions [67].

Magnetometers based on nuclear (rather than electron)

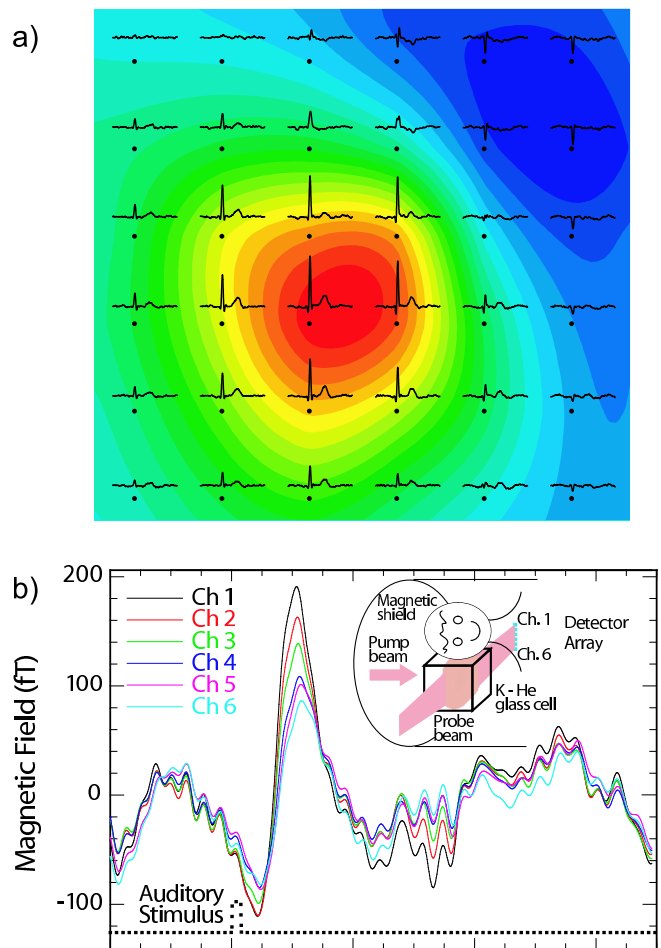


FIG. 3: Examples of biological magnetic fields recorded with atomic magnetometers. a) Time traces (averaged over 100 heartbeats) of the out-of-chest component of the magnetic field from a human heart recorded on 36 grid points spaced by 4 cm. The underlying map is a snapshot of the field distribution at the moment of strongest magnetic activity (R-peak). The scale of the map ranges from -30 pT (blue) to +60 pT (red). Figure courtesy Prof. A. Weis. b) Magnetic fields recorded from a brain in response to an auditory stimulation by a series of short clicks (averaged over about 600 presentations). The prominent feature at 100 ms after the stimulus is the evoked response in the auditory cortex, most clearly seen as a difference in the magnetic fields recorded by different channels. In contrast, ambient field drifts, such as seen before the stimulus, generate similar signals in all channels. Figure courtesy Dr. H. Xia.

spin precession also play an important role in tests of fundamental symmetries. While nuclei, such as ^3He , have a magnetic moment smaller than that of an electron by three orders of magnitude, they also display much longer spin relaxation time τ and thus can be competitive with electron-spin magnetometers in magnetic field measurements [68]. In the searches for non-magnetic spin interactions, the smallness of the nuclear magnetic moment is actually an advantage as it reduces the sensitivity to spurious magnetic effects. Measurements of nuclear spin pre-

cession of ^{199}Hg have been used to set a limit on the EDM of the mercury atom, which is also the tightest limit on an EDM of any particle. This result constrains possible violation of charge-parity (CP) symmetry due to supersymmetric particles [69]. Comparison of ^{129}Xe and ^3He precession sets the most stringent limit on the Lorentz-violating vector coupling to a nuclear spin [70, 71].

A number of new ideas for tests of fundamental symmetries using atomic magnetometers are presently being explored, such as searches for a permanent electric dipole moment using laser-cooled Cs atoms in an optical lattice [72] or an atomic fountain [73], and the possibility of using ultra-sensitive magnetometers for detecting P and T violating magnetization in solid-state samples induced by an applied electric field [74] or an internal field of a ferroelectric (see Ref. [75] and references therein).

C. Measuring magnetic fields in space

Measurements of planetary and interplanetary magnetic fields have been integral to space missions from their early days [76, 77]. The on-board instruments designed for such missions have been able to successfully meet various inherent design challenges, including the necessity to have a very broad dynamic range for the instrument, as the magnetic fields to be measured could vary by many orders of magnitude between planetary fly-bys and the craft's sojourn in interplanetary space. Other challenges include stringent requirements on reliability, the ability to withstand thermal and mechanical stresses associated with the launch and varying conditions during the flight; limited weight and size; power consumption, the ability to characterize and correct for errors due to the craft spin, etc.

Most spacecraft measuring magnetic fields currently rely on flux-gate magnetometers because of their small size and power consumption. However, optically pumped ^4He magnetometers are used in most advanced space applications because of their relative simplicity, reliability and high absolute accuracy. In a ^4He magnetometer, a weak electric discharge excites helium atoms to the metastable 2^3S_1 state, and optical pumping with a ^4He discharge lamp is employed to polarize and detect spin precession of atoms in the metastable state. Such instruments typically have sensitivity on the order of $1 - 10 \text{ pT}/\sqrt{\text{Hz}}$ and have been successfully flown on Ulysses [78] and Cassini [79, 80] missions, recently providing new information about magnetospheres of Saturn [81] and its moon Enceladus [82]. Laser-pumped ^4He magnetometers are presently being developed and have demonstrated sensitivity of $200 \text{ fT}\sqrt{\text{Hz}}$ [83] while their fundamental sensitivity limit is estimated to be about $5 \text{ fT}\sqrt{\text{Hz}}$ [84].

Deployment of more sensitive magnetometers in space will enable magnetic field measurements in weak-field space environments, as in the outer heliosphere and in the local interstellar medium. At distances from the

sun beyond about 80 astronomical units, the strength of the ambient, nominally dc, magnetic field could be as low as a few tens of picotesla (see Ref. [85] and references therein), near the limit of detectability of currently used sensors. Fluctuations of magnetic fields in space are caused by plasma process and have a bandwidth on the order of 1 Hz, corresponding to typical electron cyclotron frequency in the outer heliosphere. Atomic magnetometers are ideally suited for measurements of such fields.

D. Atomic magnetometers and nuclear magnetic resonance

One of the rapidly growing applications of atomic magnetometers is detection of NMR signals. NMR is usually detected with inductive rf pick-up coils whose sensitivity drops at low frequency, precluding many applications of low-field NMR. SQUID magnetometers have been widely used for NMR detection at low frequencies [86], but they still require cryogenic cooling, negating one of the main advantages of low-field NMR – the absence of a cryogenic superconducting magnet. Atomic magnetometers can be used in place of SQUIDS to detect the magnetic field generated by the nuclear magnetization [87, 88, 89].

One of the promising applications is “remote” NMR, where spin polarization, NMR-signal encoding and detection are performed sequentially in different parts of the apparatus [90]. Such remote NMR [91] and MRI [92] has recently been demonstrated with an atomic magnetometer.

For both remote and in-situ NMR detection, having the NMR sample and the magnetometer sensor spatially separated (as, for example, in Refs. [91, 92]) has experimental advantages, such as an ability to apply an independent, relatively strong magnetic field to the sample, which is not “seen” by the sensor if a proper geometrical arrangement is used. On the other hand, atomic magnetometers can achieve an even higher sensitivity by taking advantage of contact interactions between alkali-metal and nuclear spins. These interactions have been particularly well studied for noble gas atoms [93] and can be described by a scalar Fermi-contact interaction between the two spins. For heavy noble gases, such as ^{129}Xe , this interaction can enhance the magnetic field produced by nuclear magnetization by a large factor on the order of 600. Thus, by allowing noble gas atoms to interact directly with the alkali-metal vapor, one can obtain high sensitivity to low concentration of ^{129}Xe spins [89].

The contact interaction between nuclear and electron spins is also useful for inertial rotation sensing. Nuclear spins make good quantum gyroscopes because of their long spin coherence time, but their magnetic moment causes significant precession in stray magnetic fields [94]. An alkali-metal magnetometer can then serve two purposes, to measure the ambient magnetic field and to detect the inertial precession of nuclear spins with high

sensitivity. The requirement for magnetic field stability is rather stringent. For example, a stray magnetic field of 1 fT would cause a false spin precession rate for ^3He of about 0.04 degrees/hour, more than can be tolerated in a navigation-grade gyroscope. A SERF magnetometer can achieve this level of magnetic sensitivity, allowing it to be used for cancelation of stray magnetic fields and enabling a competitive nuclear-spin rotation sensor [95].

Another new application of atomic magnetometers is for detection of nuclear quadrupole resonance (NQR) signals. In crystalline materials nuclei with a quadrupole moment are aligned by the electric field gradient and can generate a weak rf signal following application of a resonant rf pulse. The physics of this phenomenon can be understood in the language of *alignment-to-orientation conversion* [96], a process well studied in atomic physics. For practical applications, it is particularly important that NQR signals do not average out in materials with randomly oriented crystallites such as powders. Resonance frequencies are highly material-specific and typically range from 0.1 to 5 MHz. Detection of NQR is a promising technique for identification of explosives, since most explosive materials contain the ^{14}N nuclei, possessing a large quadrupole moment. However, widespread use of NQR for this purpose has been limited due to the weakness of the NQR signals, which are typically detected with an rf coil only after substantial signal averaging [97]. Detection of weak radio-frequency signals requires modification of usual atomic-magnetometer arrangements that are designed for detection of quasi-DC magnetic fields. A tunable magnetometer for detection of weak rf field can be realized by using a bias field to tune the Zeeman energy splitting to the frequency of the rf field [18, 98]. Recently such magnetometer has been built for operation at 423 kHz with a sensitivity of 0.24 fT/Hz $^{1/2}$ and bandwidth of 600 Hz and used to detect NQR signals from ammonium nitride [99]. A detailed analysis of the fundamental limits on sensitivity of an rf atomic magnetometer [18] and an inductive pick-up coil show that atomic magnetometer has higher sensitivity up to frequencies of about 50 MHz [100].

E. Magnetometry with cold atoms

Recent breakthroughs in laser cooling and trapping have opened new avenues for precision measurements using long-lived, near-stationary collections of atoms. In particular, far-off-resonance optical traps provide a benign environment for trapping atoms with negligible photon scattering rates and storage lifetimes in excess of 300 s in an ultra-high vacuum environment [101]. Thus, the spin-coherence time of laser-cooled and trapped atoms can be substantially longer than the typical value of 1 s obtained in a buffer gas or surface-coated cell. However, due to the small volume of atom traps and limits on atomic number density from cold collisions, the total number of trapped atoms is typically on the or-

der of $10^6 - 10^8$, many orders of magnitude smaller than $10^{11} - 10^{15}$ atoms contained in a cm-sized vapor cell. While trapped atoms do not have the highest sensitivity to uniform magnetic fields, they are particularly well suited for making field measurements with high spatial resolution corresponding to the trap size, where vapor cells do not work well because spin-relaxation time quickly decreases with cell size. Such high resolution magnetic microscopes find a range of applications, from studies of magnetic domains [102] to imaging of currents on integrated circuits [103].

Two magnetometry techniques have been recently demonstrated with Rb Bose-Einstein condensates (BEC). The first involves holding the condensate in a weak magnetic trap so the energy of interaction with the magnetic field to be measured causes a perturbation of the trapping potential and changes the local atomic density [104, 105]. With a typical chemical potential in a weak magnetic trap on the order of 1 nK one gets a magnetic field sensitivity of about 1 nT. The other technique [106, 107] is similar to measurements done with hot atoms – the BEC is held in an optical dipole trap and spin precession is measured using phase-contrast imaging with an off-resonant circularly-polarized probe beam. This non-destructive imaging allows monitoring of spin precession, as shown in Fig. 4. The magnetic field sensitivity obtained with this method is 900 fT (in a single run with 250 ms integration time and an integrating area of 100 square microns). In both methods cooling atoms to quantum degeneracy improves measurement sensitivity, but whether the coherence of the BEC plays a direct role is presently an open question.

V. BRIGHT FUTURE

Recent progress in atomic magnetometry techniques can be expected to have a significant impact in four general areas. The first is the development of robust laser-pumped atomic magnetometers, largely driven by recent availability of electronically-tunable VCSEL and distributed-feedback (DFB) semiconductor lasers. Such magnetometers can replace existing discharge-lamp-pumped devices, providing higher sensitivity in geological, military, and space applications. The second area is the development of micro-fabricated mm-size magnetometers, which will open entirely new applications of magnetic monitoring in a wide range of environments. The third area is the increasing use of atomic magnetometers as sensitive detectors for weak signals, in NMR, biological applications, magnetic microscopy, and inertial rotation sensing. The fourth area is the exploration of the frontier of magnetic sensitivity, where atomic magnetometers are already surpassing SQUID sensors and can be expected to reach sensitivities significantly below 10^{-17} T/Hz $^{1/2}$. This will enable new measurements in materials science, improve the precision of fundamental physics tests, and may lead to entirely un-

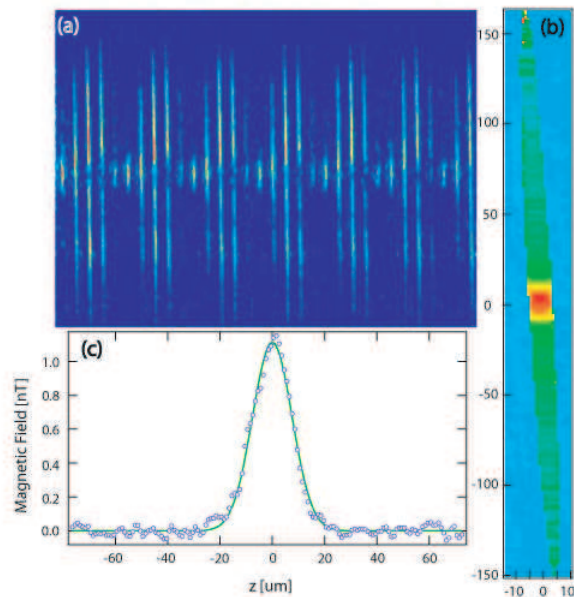


FIG. 4: Detection of effective magnetic field by imaging of Larmor precession in a Bose-Einstein condensate of ^{87}Rb [107]. The condensate contained 1.4 million atoms, optically trapped with trapping frequencies of $4.2 \text{ Hz} \times 155 \text{ Hz} \times 400 \text{ Hz}$. A uniform bias magnetic field of $16 \mu\text{T}$ is applied, while a far-detuned circularly polarized laser beam is focused onto the condensate with a waist of $7.6 \mu\text{m}$ to simulate the effects of an additional localized magnetic field. Part (a) shows a sequence of 32 individual normalized atomic-spin-sensitive phase-contrast images taken after an evolution time of 50 ms and spaced in time by $100 \mu\text{s}$. The variation of the brightness of the images with a period of ≈ 5 frames is due to Larmor precession of the atomic spins. Part (b) shows a pseudocolor map of the phase of Larmor precession as a function of position in microns. The phase corresponds to the effective magnetic field shown in Part (c) as a function of position in the central portion of the condensate, demonstrating the high resolution and precision of the technique. The gaussian phase shift follows the intensity profile of the far-detuned laser beam, and the solid line is a fit to this profile. Figure courtesy Drs. M. Vengalattore and J. Higbie.

expected discoveries. The future of measuring magnetic fields with atoms and light is indeed bright.

Acknowledgments

This work is supported by DOD MURI grant # N-00014-05-1-0406. We are grateful to E. Alexandrov, M. Balabas, G. Bison, S. Bale, W. Gawlik, J. Higbie, M. Ledbetter, I. M. Savukov, D. Stamper-Kurn, A. Sushkov, M. Vengalattore, and A. Weis for providing valuable input for this review.

-
- [1] H. Dehmelt, Phys. Rev. **105**, 1924 (1957).
 - [2] W. Bell and A. Bloom, Phys. Rev. **107**, 1559 (1957).
 - [3] W. Bell and A. Bloom, Phys. Rev. Lett. **6**, 280 (1961).
 - [4] J. Dupont-Roc, S. Haroche, and C. Cohen-Tannoudji, Phys. Lett. A **28a**, 638 (1969).
 - [5] J. Dupont-Roc, Rev. Phys. Appl. **5**, 853 (1970).
 - [6] D. Budker, W. Gawlik, D. F. Kimball, S. M. Rochester, V. V. Yashchuk, and A. Weis, Rev. Mod. Phys. **74**, 1153 (2002).
 - [7] E. B. Alexandrov, M. Auzinsh, D. Budker, D. F. Kimball, S. M. Rochester, and V. V. Yashchuk, J. Opt. Soc. Am. B **22**, 7 (2005).
 - [8] E. B. Aleksandrov, M. V. Balabas, A. K. Vershovskii, and A. S. Pazgalev, Technical Physics **49**, 779 (2004).
 - [9] H. Gilles, J. Hamel, and B. Cheron, Rev. Sci. Instrum. **72**, 2253 (2001).
 - [10] A. Weis and R. Wynands, Optics and Lasers in Engineering **43**, 387 (2005).
 - [11] D. Budker, D. F. Kimball, S. M. Rochester, V. V. Yashchuk, and M. Zolotarev, Phys. Rev. A **62**, 043403 (2000).
 - [12] I. K. Kominis, T. W. Kornack, J. C. Allred, and M. V. Romalis, Nature **422**, 596 (2003).
 - [13] J. Clarke, in *SQUID Sensors: Fundamentals, Fabrication, and Applications*, edited by H. Weinstock (Kluwer Academic, The Netherlands, 1996), pp. 1–62.
 - [14] S. Groeger, A. S. Pazgalev, and A. Weis, Appl. Phys. B. **80**, 645 (2005).

- [15] A. K. Vershovskii, A. S. Pazgalev, and E. B. Aleksandrov, *Technical Physics* **45**, 88 (2000).
- [16] G. M. Geremia, J. K. Stockton, and H. Mabuchi, *Phys. Rev. Lett.* **94**, 203002 (2005).
- [17] M. Auzinsh, D. Budker, D. F. Kimball, S. Rochester, J. E. Stalnaker, A. O. Sushkov, and V. Yashchuk, *Phys. Rev. Lett.* **93**, 173002 (2004).
- [18] I. M. Savukov, S. J. Seltzer, M. V. Romalis, and K. L. Sauer, *Phys. Rev. Lett.* **95**, 0630041 (2005).
- [19] W. Happer and B. Mathur, *Phys. Rev.* **163**, 12 (1967).
- [20] M. Fleischhauer, A. B. Matsko, and M. O. Scully, *Phys. Rev. A* **62**, 013808/1 (2000).
- [21] I. Novikova, A. B. Matsko, V. L. Velichansky, M. O. Scully, and G. R. Welch, *Phys. Rev. A* **63**, 063802/1 (2001).
- [22] H. Robinson, E. Ensberg, and H. Dehmelt, *Bull. Am. Phys. Soc.* **3**, 9 (1958).
- [23] M. A. Bouchiat and J. Brossel, *Phys. Rev.* **147**, 41 (1966).
- [24] V. A. Sautenkov, M. D. Lukin, C. J. Bednar, I. Novikova, E. Mikhailov, M. Fleischhauer, V. L. Velichansky, G. R. Welch, and M. O. Scully, *Phys. Rev. A* **62**, 023810/1 (2000).
- [25] E. B. Alexandrov, M. V. Balabas, D. Budker, D. English, D. F. Kimball, C. H. Li, and V. V. Yashchuk, *Phys. Rev. A* **66**, 042903/1 (2002).
- [26] W. Happer and H. Tang, *Phys. Rev. Lett.* **31**, 273 (1973).
- [27] W. Happer and A. C. Tam, *Phys. Rev. A* **16**, 1877 (1977).
- [28] R. H. Dicke, *Phys. Rev.* **89**, 472 (1953).
- [29] I. M. Savukov and M. V. Romalis, *Phys. Rev. A* **71**, 23405 (2005).
- [30] C. J. Erickson, D. Levron, W. Happer, S. Kadlecsek, B. Chann, L. W. Anderson, and T. G. Walker, *Phys. Rev. Lett.* **85**, 4237 (2000).
- [31] S. Kadlecsek, L. W. Anderson, and T. G. Walker, *Phys. Rev. Lett.* **80**, 55125515 (1998).
- [32] J. Allred, R. Lyman, T. Kornack, and M. Romalis, *Phys. Rev. Lett.* **89**, 130801 (2002).
- [33] S. Seltzer and M. V. Romalis, *Appl. Phys. Lett.* **85**, 4804 (2004).
- [34] S. Appelt, A. Ben-Amar Baranga, A. R. Young, and W. Happer, *Phys. Rev. A* **59**, 2078 (1999).
- [35] Y. Y. Jau, A. B. Post, N. N. Kuzma, A. M. Braun, M. V. Romalis, and W. Happer, *Phys. Rev. Lett.* **92**, 110801/1 (2004).
- [36] S. J. Smullin, I. M. Savukov, G. Vasilakis, R. K. Ghosh, and M. V. Romalis, <http://arxiv.org/abs/physics/0611085> (2006).
- [37] A. Bloom, *Appl. Opt.* **1**, 61 (1962).
- [38] M. Stahler, S. Knappe, C. Affolderbach, W. Kemp, and R. Wynands, *Europhys. Lett.* **54**, 323 (2001).
- [39] V. Acosta, M. P. Ledbetter, S. M. Rochester, D. Budker, D. F. Jackson-Kimball, D. C. Hovde, W. Gawlik, S. Pustelny, and J. Zachorowski, *Phys. Rev. A* **73**, 053404 (2006).
- [40] C. Andreeva, G. Bevilacqua, V. Biancalana, S. Cartaleva, Y. Dancheva, T. Karaulanov, C. Marinelli, E. Mariotti, and L. Moi, *Appl. Phys. B, Lasers Opt.* **76**, 667 (2003).
- [41] E. Alipieva, C. Andreeva, L. Avramov, G. Bevilacqua, V. Biancalana, E. Borisova, E. Breschi, S. Cartaleva, Y. Dancheva, S. Gateva, et al., *Proceedings of SPIE* **5830**, 170 (2005).
- [42] S. J. Seltzer, P. J. Meares, and M. V. Romalis, [physics/0611014](http://arxiv.org/abs/physics/0611014) (2006).
- [43] E. B. Alexandrov, A. S. Pazgalev, and J. L. Rasson, *Opt. Spectrosc.* **82**, 14 (1997).
- [44] V. V. Yashchuk, D. Budker, W. Gawlik, D. F. Kimball, Y. P. Malakyan, and S. M. Rochester, *Phys. Rev. Lett.* **90**, 253001 (2003).
- [45] S. Pustelny, D. F. J. Kimball, S. M. Rochester, V. V. Yashchuk, W. Gawlik, and D. Budker, *Phys. Rev. A* **73**, 023817 (2006).
- [46] M. B. Weissman, *Rev. Mod. Phys.* **60**, 537571 (1988).
- [47] Z. Li, R. T. Wakai, and T. G. Walker, *Appl. Phys. Lett.* **89**, 134105 (2006).
- [48] E. B. Alexandrov, M. V. Balabas, V. N. Kulyasov, A. E. Ivanov, A. S. Pazgalev, J. L. Rasson, A. K. Vershovskii, and N. N. Yakobson, *Meas. Sci. Technol. (UK)* **15**, 918 (2004).
- [49] O. Gravrand, A. Khokhlov, J. L. L. Mouel, and J. M. Leger, *Earth Planets Space* **53**, 949 (2001).
- [50] A. B. Matsko, D. Strekalov, and L. Maleki, *Opt. Commun.* **247**, 141 (2005).
- [51] P. D. D. Schwindt, L. Hollberg, and J. Kitching, *Rev. Sci. Instrum.* **76**, 126103 (2005).
- [52] J. Higbie, E. Corsini, and D. Budker, *Rev. Sci. Instrum.* (2006).
- [53] J. Bechhoefer, *Rev. Mod. Phys.* **77**, 783 (2005).
- [54] D. C. Rife and R. R. Boorstyn, *IEEE Trans. Inform. Theory* **20**, 591 (1974).
- [55] M. V. Balabas, D. Budker, J. Kitching, P. D. D. Schwindt, and J. E. Stalnaker, *J. Opt. Soc. Am. B, Opt. Phys.* **23**, 1001 (2006).
- [56] P. D. D. Schwindt, S. Knappe, V. Shah, L. Hollberg, J. Kitching, L. A. Liew, and J. Moreland, *Appl. Phys. Lett.* **85**, 6409 (2004).
- [57] S. Knappe, P. D. D. Schwindt, V. Gerginov, V. Shah, L. Liew, J. Moreland, H. G. Robinson, L. Hollberg, and J. Kitching, *Journal of Optics A: Pure and Applied Optics* **8**, S318 (2006).
- [58] S. Pustelny, D. F. J. Kimball, S. M. Rochester, V. V. Yashchuk, and D. Budker, *Phys. Rev. A (physics/0608109)* (2006).
- [59] R. Fenici, D. Brisinda, and A. M. Meloni, *Expert Review of Molecular Diagnostics* **5**, 291 (2005).
- [60] M. Hämäläinen, R. Hari, R. J. Ilmoniemi, J. Knuutila, and O. V. Lounasmaa, *Rev. Mod. Phys.* **65**, 413497 (1993).
- [61] A. C. Papanicolaou, E. M. Castillo, R. Billingsley-Marshall, E. Patariaia, and P. G. Simos, *International Review of Neurobiology* **68**, 223 (2005).
- [62] M. N. Livanov, A. N. Kozlov, A. V. Korinevskii, V. P. Markin, S. E. Sinelnikova, and I. A. Kholodov, *Doklady Akademii Nauk SSSR* **238**, 253 (1977).
- [63] G. Bison, R. Wynands, and A. Weis, *Appl. Phys. B* **76**, 325 (2003).
- [64] H. Xia, A. B. Baranga, D. Hoffman, and M. V. Romalis, *Appl. Phys. Lett.* (2006).
- [65] S. A. Murthy, J. Krause, D., Z. L. Li, and L. R. Hunter, *Phys. Rev. Lett.* **63**, 965 (1989).
- [66] C. J. Berglund, L. R. Hunter, J. Krause, D., E. O. Prigge, M. S. Ronfeldt, and S. K. Lamoreaux, *Phys. Rev. Lett.* **75**, 1879 (1995).
- [67] A. N. Youdin, J. Krause, D., K. Jagannathan, L. R. Hunter, and S. K. Lamoreaux, *Phys. Rev. Lett.* **77**, 2170 (2006).

- (1996).
- [68] H. Gilles, Y. Monfort, and J. Hamel, *Rev. Sci. Instrum.* **74**, 4515 (2003).
 - [69] M. V. Romalis, W. C. Griffith, J. P. Jacobs, and E. N. Fortson, *Phys. Rev. Lett.* **86**, 2505 (2001).
 - [70] D. Bear, R. E. Stoner, R. L. Walsworth, V. A. Kosteleck, and C. D. Lane, *Phys. Rev. Lett.* **85**, 5038 (2000).
 - [71] D. Bear, R. E. Stoner, R. L. Walsworth, V. A. Kosteleck, and C. D. Lane, *Phys. Rev. Lett.* **89**, 209902 (2002).
 - [72] C. Chin, V. Leiber, V. Vuletic, A. J. Kerman, and S. Chu, *Phys. Rev. A* **63**, 0334011 (2001).
 - [73] J. M. Amini, C. T. M. Jr., and H. Gould, <http://arxiv.org/physics/0602011> (2006).
 - [74] S. K. Lamoreaux, *Phys. Rev. A* **66**, 022109 (2002).
 - [75] D. Budker, S. K. Lamoreaux, A. O. Sushkov, and O. P. Sushkov, *Phys. Rev. A* **73**, 022107 (2006).
 - [76] N. F. Ness, *Space Sci. Rev. (Netherlands)* **11**, 459 (1970).
 - [77] M. H. Acuna, in *Encyclopedia of planetary sciences*, edited by J. H. Shirley and R. W. Fairbridge (Chapman & Hall, London, 1997).
 - [78] A. Balogh, in *IEE Colloquium on 'Satellite Instrumentation'* (IEE, London, UK, 1988), vol. Digest No.12, pp. 2/1–3.
 - [79] D. J. Southwood, A. Balogh, and E. J. Smith, *J. Br. Interplanet. Soc. (UK)* **45**, 371 (1992).
 - [80] M. W. Dunlop, M. K. Dougherty, S. Kellock, and D. J. Southwood, *Planet. Space Sci. (UK)* **47**, 1389 (1999).
 - [81] M. K. Dougherty, N. Achilleos, N. Andre, C. S. Arridge, A. Balogh, C. Bertucci, M. E. Burton, S. W. H. Cowley, G. Erdos, G. Giampieri, et al., *Science* **307**, 1266 (2005).
 - [82] M. K. Dougherty, K. K. Khurana, F. M. Neubauer, C. T. Russell, J. Saur, J. S. Leisner, and M. E. Burton, *Science* **311**, 1406 (2006).
 - [83] R. E. Slocum, G. Kuhlman, L. Ryan, and D. King, in *Oceans 2002* (IEEE. Conference Proceedings (Cat. No.02CH37362)., 2002), vol. 2, pp. 945–51.
 - [84] D. D. McGregor, *Rev. Sci. Instrum.* **58**, 1067 (1987).
 - [85] L. F. Burlaga, N. F. Ness, C. Wang, J. D. Richardson, F. B. McDonald, and E. C. Stone, *Astrophysical Journal* **618**, 10741078 (2005).
 - [86] Y. S. Greenberg, *Rev. Mod. Phys.* **70**, 175 (1998).
 - [87] C. Cohen-Tannoudji, J. DuPont-Roc, S. Haroche, and F. Laloe, *Phys. Rev. Lett.* **22**, 758 (1969).
 - [88] V. V. Yashchuk, J. Granwehr, D. F. Kimball, S. M. Rochester, A. H. Trabesinger, J. T. Urban, D. Budker, and A. Pines, *Phys. Rev. Lett.* **93**, 160801 (2004).
 - [89] I. M. Savukov and M. V. Romalis, *Phys. Rev. Lett.* **94**, 1230011 (2005).
 - [90] A. J. Moulé, M. M. Spence, S. Han, J. A. Seeley, K. L. Pierce, S. Saxena, and A. Pines, *Proc. Natl. Acad. Sci. U. S. A* **100**, 9122 (2003).
 - [91] S. Xu, S. M. Rochester, V. V. Yashchuk, M. H. Donaldson, and D. Budker, *Rev. Sci. Instrum.* **77**, 083106 (2006).
 - [92] S. Xu, V. V. Yashchuk, M. H. Donaldson, S. M. Rochester, D. Budker, and A. Pines, *Proc. Natl. Acad. Sci. U. S. A* p. 0605396103 (2006).
 - [93] S. R. Schaefer, G. D. Cates, T.-R. Chien, D. Gonatas, W. Happer, and T. G. Walker, *Phys. Rev. A* **39**, 5613 (1989).
 - [94] K. F. Woodman, P. W. Franks, and M. D. Richards, *Journal of Navigation* **40**, 366 (1987).
 - [95] T. W. Kornack, R. K. Ghosh, and M. V. Romalis, *Phys. Rev. Lett.* **95**, 230801 (2005).
 - [96] D. Budker, D. F. Kimball, S. M. Rochester, and J. T. Urban, *Chem. Phys. Lett.* **378**, 440 (2003).
 - [97] A. N. Garroway, M. L. Buess, J. B. Miller, B. H. Suits, A. D. Hibbs, G. A. Barrall, R. Matthews, and L. J. Burnett, *IEEE Trans. Geosci. Remote Sens. (USA)* **39**, 1108 (2001).
 - [98] M. P. Ledbetter, V. M. Acosta, S. M. Rochester, D. Budker, S. Pustelny, and V. V. Yashchuk, *physics/0609196* (2006).
 - [99] S.-K. Lee, K. L. Sauer, S. J. Seltzer, O. Alem, and M. V. Romalis, *Appl. Phys. Lett.* (**in press**) (2006).
 - [100] I. M. Savukov, S. J. Seltzer, and M. V. Romalis, *Submitted* (2006).
 - [101] K. M. O'Hara, S. R. Granade, M. E. Gehm, T. A. Savard, S. Bali, C. Freed, and J. E. Thomas, *Phys. Rev. Lett.* **82**, 4204 (1999).
 - [102] M. R. Freeman and B. C. Choi, *Science* **294**, 1484 (2001).
 - [103] S. Chatrathorn, E. F. Fleet, F. C. Wellstood, L. A. Knauss, and T. M. Eiles, *Appl. Phys. Lett.* **76**, 2304 (2000).
 - [104] S. Wildermuth, S. Hofferberth, I. Lesanovsky, E. Haller, L. M. Andersson, S. Groth, I. Bar-Joseph, P. Kruger, and J. Schmiedmayer, *Nature* **435**, 440 (2005).
 - [105] S. Wildermuth, S. Hofferberth, I. Lesanovsky, S. Groth, P. Krger, J. Schmiedmayer, and I. Bar-Joseph, *Appl. Phys. Lett.* **88**, 264103 (2006).
 - [106] J. M. Higbie, L. E. Sadler, S. Inouye, A. P. Chikkatur, S. R. Leslie, K. L. Moore, V. Savalli, and D. Stamper-Kurn, *Phys. Rev. Lett.* **95**, 0504011 (2005).
 - [107] M. Vengalattore, J. M. Higbie, L. E. Sadler, S. R. Leslie, and D. Stamper-Kurn (2006), to be submitted.